Upregulation of anti-apoptotic factors in upper motor neurons after spinal cord injury in adult zebrafish

Kazuhiro Ogai[a], Suguru Hisano[b], Kazuhiro Mawatari[a], Kayo Sugitani[a], Yoshiki Koriyama[c], Hiroshi Nakashima[a], Satoru Kato[c,*]

[a]Division of Health Sciences, Graduate School of Medical Science, Kanazawa University, 5-11-80 Kodatsuno, Kanazawa, Ishikawa 9200942, Japan

[b]Department of Laboratory Sciences, School of Health Sciences, College of Medical, Pharmaceutical and Health Sciences, Kanazawa University, 5-11-80 Kodatsuno, Kanazawa, Ishikawa 9200942, Japan

[c]Department of Molecular Neurobiology, Graduate School of Medical Science, Kanazawa University, 13-1 Takaramachi, Kanazawa, Ishikawa 9208640, Japan

Running title

Anti-apoptotic reactions after spinal cord injury in zebrafish brain

*All correspondence should be addressed to:

Satoru Kato

Department of Molecular Neurobiology, Graduate School of Medical Science, Kanazawa University, 13-1 Takaramachi, Kanazawa, Ishikawa 9208640, Japan

Tel.: +81 76 265 2450; Fax: +81 76 234 4325

E-mail: satoru@med.m.kanazawa-u.ac.jp

Abstract

Unlike mammals, fish motor function can recover within 6–8 weeks after spinal cord injury (SCI). The motor function of zebrafish is regulated by dual control; the upper motor neurons of the brainstem and motor neurons of the spinal cord. In this study, we aimed to investigate the framework behind the regeneration of upper motor neurons in adult zebrafish after SCI. In particular, we investigated the cell survival of axotomized upper motor neurons and its molecular machinery in zebrafish brain. As representative nuclei of upper motor neurons, we retrogradely labeled neurons in the nucleus of medial longitudinal fasciculus (NMLF) and the intermediate reticular formation (IMRF) using a tracer injected into the lesion site of the spinal cord. Four to eight neurons in each thin sections of the area of NMLF and IMRF were successfully traced at least 1–15 days after SCI. TUNEL staining and BrdU labeling assay revealed that there was no apoptosis or cell proliferation in the axotomized neurons of the brainstem at various time points after SCI. In contrast, axotomized neurons labeled with a neurotracer showed increased expression of anti-apoptotic factors, such as Bcl-2 and phospho-Akt (p-Akt), at 1–6 days after SCI. Such a rapid increase of Bcl-2 and p-Akt protein levels after SCI was quantitatively confirmed by western blot analysis. These data strongly indicate that upper motor neurons in the NMLF and IMRF can survive and regrow their axons into the spinal cord through the rapid activation of anti-apoptotic molecules after SCI. The regrowing axons from upper motor neurons reached the lesion site at 10–15 days and then crossed at 4–6 weeks after SCI. These long-distance descending axons from originally axotomized neurons have a major role in restoration of motor function after SCI.

Key words

spinal cord regeneration; zebrafish; upper motor neuron; Bcl-2; p-Akt; cell survival

Abbreviations

Bcl-2, B-cell lymphoma 2; BrdU, 5-bromo-2′-deoxyuridine; CNS, central nervous system; DAPI, 4′, 6-diamidino-2-phenylindole; dpl, day(s) post-lesion; dUTP, deoxyuridine triphosphate; GAP43, growth associated protein 43; IMRF, intermediate reticular formation; NMLF, nucleus of medial longitudinal fasciculus; RDA, rhodamine dextran amine; SCI, spinal cord injury; TUNEL, terminal deoxynucleotidyl transferase-mediated dUTP nick end labeling

1. Introduction

In general, mammalian central neurons cannot repair after nerve injury, whereas fish central neurons can regrow their axons and restore function even after nerve transection. In the rat model of spinal cord lesion, primary cortical motor neurons and motor neurons in the spinal cord become apoptotic and are lost within 1 week after spinal cord injury (SCI) (Hains et al., 2003). Conversely, zebrafish can regenerate axons of motor neurons and recover motor function 6–8 weeks after SCI (Van Raamsdonk et al., 1998; Becker et al., 2004). Similar to mammals, motor function in zebrafish is controlled by motor neurons from two distinct populations, the brainstem and the spinal cord. Recently, it was reported that motor neurons in the spinal cord are newly-generated from progenitor cells located around the central canal after SCI (Reimer et al., 2008). These neurons extend axons to reinnervate their target organs. A pioneering work by Becker et al. (1997) reported that the neurons in about 20 brain regions were retrogradely labeled with a tracer injected into the lesion site of the spinal cord. Among the 20 brain regions, there were brain nuclei with a high axonal regenerative capacity, such as the nucleus of the medial longitudinal fasciculus (NMLF) and the intermediate reticular formation (IMRF). In these brain nuclei, 32–51% of the neurons regenerate their axons into the spinal cord. In brain nuclei of lower axonal regenerative capacity, such as the nucleus ruber and the nucleus of the lateral lemniscus, only 11–15% of the neurons regenerate their spinal axons (Becker et al., 1997). They also reported that zebrafish brainstem neurons, which were retrogradely double-labeled by tracers, could be observed 6 weeks after SCI. These data indicate that upper motor neurons in the brainstem can survive for a long time and then regrow their axons to the spinal cord after SCI. However, there are three questions that should be solved in more detail: (1) Are the regenerating axons derived only from originally axotomized and

survived neurons or in part from newly-generated neurons? (2) Do the cell apoptosis and/or cell proliferation in the brainstem occur during the axonal regeneration process? (3) What kind of molecule is responsible for cell survival of upper motor neurons after SCI? In the present study, therefore, we focused on these specific questions, especially on elucidating the molecular machinery for cell survival of upper motor neurons following SCI. To answer these questions, we conducted terminal deoxynucleotidyl transferase-mediated dUTP nick end labeling (TUNEL) assay, 5-bromo-2′-deoxyuridine (BrdU) labeling and immunohistochemical staining of anti-apoptotic factors (Bcl-2 and phospho-Akt) in combination with retrograde tracing technique in adult zebrafish after SCI.

2. Materials and Methods

2.1. Animals

Adult zebrafish (*Danio rerio*; 3–4 cm in body length) were used throughout this study. The experiments were performed in accordance with the Committee on Animal Experimentation of the Kanazawa University, and all attention was paid to minimize pain and the numbers of fish used.

2.2. Spinal cord injury

As described previously (Reimer et al., 2009), fish were anesthetized by immersion in 0.033% ethyl 3-aminobenzoate methanesulfonic acid (MS222; Sigma-Aldrich, St. Louis, MO, USA) in 0.01 M phosphate buffered saline (PBS; pH 7.4), and the spinal cord was transected 4 mm caudal to the brainstem-spinal cord junction, unless otherwise specified. After surgery, the incision was sealed with histoacryl (B. Braun Melsungen AG, Melsungen, Germany) and the fish were reared in 26 °C water until appropriate time points.

2.3. Tissue preparation

At appropriate time points, the brain and the spinal cord were exposed under deep anesthesia (0.1% MS222 in PBS) and fixed with 4% paraformaldehyde in PBS, overnight at 4 °C. They were then incubated in an ascending series of sucrose concentrations from 5 to 20%, and embedded in optimal cutting temperature (OCT) compound (Sakura Finetek, Tokyo, Japan). Subsequently, cryosections were prepared at 12 or 20 μm thickness. The coronal sections were used for all experiments of the brainstem and the longitudinal sections were used for experiments of the spinal cord. To determine the anatomical structure of the adult zebrafish brainstem, we referred to the

zebrafish brain atlas (Wullimann et al., 1996).

2.4. Retrograde tracing

To label brainstem neurons projecting into the spinal cord, retrograde tracing from the lesion site of the spinal cord was performed as described previously (Becker et al., 1997). In brief, a small piece of gelatin foam (Spongel; Astellas, Tokyo, Japan) soaked with 25 mg/ml biocytin (Sigma-Aldrich, St. Louis, MO, USA) or 50 mg/ml rhodamine dextran amine (RDA, Fluororuby; Fluorochrome, Denver, CO, USA) was applied to the transected spinal cord. The tracer was allowed to be transported to the brainstem neurons for at least 1 day (biocytin), or 3–6 days (RDA). Biocytin was detected with DyLight 594-conjugated NeutrAvidin (Thermo Scientific, Waltham, MA, USA) along with the appropriate secondary antibody for immunohistochemistry (see section 2.8). RDA was directly detected by fluorescence microscopy (VB-7000; Keyence, Osaka, Japan).

2.5. TUNEL assay

Apoptotic cells were detected by TUNEL technology using *In Situ* Cell Death Detection Kit, Fluorescein (Roche Applied Science, Mannheim, Germany) according to the manufacturer's instructions. In brief, sections were microwaved in 0.01 M citrate buffer, washed, blocked and incubated with terminal deoxynucleotidyl transferase and fluorescein-conjugated dUTP at 37 °C overnight, followed by counter-staining with 2 μg/ml 4′, 6-diamidino-2-phenylindole (DAPI; Wako Pure Chemical Industries, Osaka, Japan). Positive cells were visualized by fluorescence microscopy. For the positive control, 100 U/ml DNase I (Takara Bio, Shiga, Japan) was applied to the sections prior to TUNEL staining.

2.6. Intraperitoneal application of BrdU

BrdU incorporation assay was performed to visualize cell proliferation, as described previously (Reimer et al., 2008). In brief, fish were anesthetized and intraperitoneally injected with 50 µl of 2.5 mg/ml BrdU (Sigma-Aldrich) at 0, 2 and 4 days post-lesion (dpl). Cells incorporating BrdU were visualized by immunohistochemistry (see section 2.8).

2.7. Hematoxylin-eosin staining

Hematoxylin-eosin staining was carried out to show the structure of lesioned spinal cord as follows. Sections were stained with Mayer's hematoxylin (Wako Pure Chemical Industries) for 3 minutes followed by washing and counter-staining with 1% eosin-Y (Wako Pure Chemical Industries) for 10 minutes. After dehydration in an ascending series of ethanol concentrations from 50 to 100%, sections were cleared in xylene and mounted with MGK-S (Matsunami Glass, Osaka, Japan). The sections were then observed by bright field microscopy (VB-7000).

2.8. Immunohistochemistry

Primary antibodies used were as follows; mouse anti-BrdU (Sigma-Aldrich; 1:500), rabbit anti-Bcl-2 (Santa Cruz Biotechnology, Santa Cruz, CA, USA; 1:300), rabbit anti-phospho-Akt (p-Akt; $pSer^{473}$) (Sigma-Aldrich; 1:500) and mouse anti-GAP43 (Santa Cruz Biotechnology; 1:300). Immunohistochemistry was performed as described previously (Matsukawa et al., 2004; Nagashima et al., 2009). In brief, antigen retrieval was performed by autoclaving sections at 121 °C for 20 min in 0.01 M citrate buffer (pH 6.0) for Bcl-2, p-Akt and GAP43 immunohistochemistry, or

incubating sections with 2 M HCl at 37 °C for 30 min for BrdU immunohistochemistry. Sections were then washed, blocked and incubated with primary antibodies overnight at 4 °C. After washing, sections were incubated with the appropriate Alexa Fluor 488-conjugated secondary antibodies at 23 °C for 1 hour, followed by washing and nuclear staining with 2 μg/ml DAPI. The sections were then observed by fluorescence microscopy. Obtained images were contrast-adjusted and color-overlaid using Photoshop CS5 software (Adobe Systems, San Jose, CA, USA).

2.9. Western blot analysis

At appropriate time-points, the brains minus the telencephalon and the optic tectum, where the projections to the spinal cord were absent (Becker et al., 1997), were extracted and sonicated in 100 μl lysis buffer (10 mM 4-(2-hydroxyethyl)-1-piperazineethanesulfonic acid (HEPES; pH 7.4), 150 mM NaCl, 0.5% Triton X-100, 50 mM sodium fluoride and 1 mM sodium orthovanadate: purchased from Wako Pure Chemical Industries or Nacalai Tesque, Kyoto, Japan). The supernatants were collected and the protein concentration was measured using the Bradford method (Bio-Rad, Hercules, CA, USA). 30 μg of total protein was loaded in each lane of a 15% sodium dodecyl sulfate polyacrylamide gel, and transferred to a nitrocellulose membrane (Whatman, Maidstone, UK). The membrane was cut at the 47 kDa protein marker (Nacalai Tesque) and separated into two parts to probe for Bcl-2 (1:500, 26 kDa) and p-Akt (1:500, 56 kDa). Primary antibodies used were the same as those used in the immunohistochemistry (see section 2.8). After washing and incubation with alkaline phosphatase-conjugated secondary antibody (Sigma), the signals were visualized by BCIP/NBT Phosphatase Substrate System (KPL, Gaithersburg, MD, USA). Densitometrical analysis was performed using ImageJ software (National

Institutes of Health, Bethesda, MD, USA).

2.10. Cell counting

The number of Bcl-2- or p-Akt-immunoreactive cells in the NMLF and IMRF was counted after immunohistochemistry (see section 2.8) using serial brain sections in which the whole region of the NMLF and IMRF was included. We used 20 μm-thick sections to minimize double-counting due to the cell splitting, because the cell diameter of upper motor neurons was not much larger than 20 μm (Becker et al., 1997). In addition, the cells without DAPI signal (i.e., counterpart of the split cell) were excluded from the counting. The anatomical position was determined by the same procedure as in section 2.3. For counting, at least 3 animals in each group were recruited. After counting the cells, means and SEMs were calculated on all animals ($n \geq 3$).

2.11. Behavioral analysis

To quantify the restoration of motor function, behavioral analysis was performed with a slight modification of previously described method (Kato et al., 1996; Kato et al., 2004; Kaneda et al., 2008). In brief, a single zebrafish was placed in a water tank (370 mm × 240 mm, water depth = 80 mm) and its spontaneous movement was captured by two video cameras (EVI-1011; Sony, Tokyo, Japan) placed both on the top and at the side of the tank for 5 min at 30 frames/sec. The position of the fish in each frame was determined, and the three-dimensional coordination of the fish was then reconstructed by combining two images (from the top and side view) with previously developed software (Kato et al., 1996; Kato et al., 2004; Kaneda et al., 2008) on a computer (Precision 490; Dell, Round Rock, TX, USA). The total distance of swimming was calculated as described in Kato et al. (1996). At least 3 fish were

recruited for each time point after SCI.

2.12. Statistical analysis

The levels of Bcl-2 or p-Akt protein in brainstem neurons at various time points after SCI were quantified densitometrically and expressed as a ratio compared with an unlesioned fish. The number of Bcl-2- and p-Akt-positive cells was expressed as the means ± SEM, and statistical significance was evaluated by the Student's *t*-test using Origin software (version 8; OriginLab, Northampton, MA, USA). Total distance of swimming for 5 min was expressed as the means ± SEM, and statistical significance was evaluated using the one-way ANOVA followed by Tukey's *post hoc* test using Origin software.

3. Results

← Fig. 1

3.1. Stability of neurotracers in brainstem neurons after SCI

In this study, we transected the spinal cord of zebrafish 4 mm caudal to brainstem-spinal cord junction, unless otherwise specified. Retrograde labeling of the NMLF and IMRF nuclei in the brainstem was performed by placing gelatin foam soaked with rhodamine dextran amine (RDA) or biocytin at the transection site in the spinal cord (Becker et al., 2004). In the area of NMLF (Fig. 1A), approximately 10 RDA-labeled neurons were seen at 1 day post-lesion (dpl). The intense signal of RDA was sustained for at least 3–6 dpl (Figs. 1B–D). In the area of IMRF (Fig. 1E), similar stable labeling of RDA could be seen in 1–6 dpl (Figs. 1F–H). In both areas, retrogradely labeled neurons were detected even at 15 dpl (data not shown). In contrast, retrograde labeling with biocytin was a slightly more labile. Stable labeling with biocytin could be seen only to 3 dpl in the NMLF and IMRF (data not shown). Therefore, we used RDA for long-term experiments over 6 dpl and biocytin for short-term experiments up to 3 dpl. The long-term presence of neurons in the NMLF and IMRF labeled by the retrograde tracer strongly indicates that these neurons survive after SCI.

← Fig. 2

3.2. Absence of apoptosis in axotomized brainstem neurons following SCI

To further elucidate the survival of brainstem neurons after SCI, we conducted TUNEL assay in NMLF and IMRF neurons identified by retrograde labeling with RDA at 6 dpl. In these neurons, there were no double positive neurons with TUNEL-positive ($TUNEL^+$) and $tracer^+$ at 6 dpl (Fig. 2). The positive control treated with DNase I

yielded clearly positive cells (data not shown). Thus, axotomized neurons in the NMLF and IMRF could avoid undergoing apoptosis at least 6 days after SCI.

← Fig. 3

3.3. Absence of cell proliferation in the brainstem following SCI

In axonal regeneration of the central nervous system (CNS), there are two possibilities for the cellular origin of regenerating axons after nerve injury. They can either be derived from newly-generated neurons or the neurons themselves could have survived after nerve injury. To determine which cell types are present in the brainstem of adult zebrafish during axonal regeneration after SCI, we performed a BrdU incorporation assay. BrdU was intraperitoneally injected at 0, 2 and 4 dpl (Figs. 3A and H). To confirm successful incorporation of BrdU, we chose the paraventricular zone in the telencephalon as a positive control, as many neural precursor cells are present even in the adult zebrafish (Kizil et al., 2012). $BrdU^+$ cells could be detected in this region at 7 dpl (Figs. 3B and C) and at 6 weeks post-lesion (Figs. 3J and K). However, no $BrdU^+$ neurons were seen both in the NMLF (Figs. 3D and E) and IMRF (Figs. 3F and G) at 7 dpl.

At 6 weeks post-lesion, the spinal cord was transected 4 mm caudal to the primary lesion site to retrogradely label brainstem neurons with biocytin. Brain sections were prepared 1 day after labeling and immunohistochemistry was performed for BrdU detection along with biocytin tracing (Figs. 3H and I). Neither $BrdU^+$ neurons nor $BrdU^+$/$biocytin^+$ double-positive neurons could be observed both in the NMLF (Figs. 3L–N) and IMRF (Figs. 3O–Q) at 6 weeks after SCI.

← Figs. 4 and 5

3.4. Upregulation of anti-apoptotic factors in axotomized brainstem neurons after SCI

To ascertain the molecules regulating cell-survival of zebrafish brainstem neurons after SCI, we performed a western blot analysis of the anti-apoptotic factors Bcl-2 and phospho-Akt (p-Akt) in the total protein extracts from the brainstem, including the NMLF and IMRF. In parallel, we performed immunohistochemistry for Bcl-2 and p-Akt in the NMLF and IMRF along with retrograde labeling at 3 and 6 dpl. Bcl-2 protein levels in the brainstem, including the NMLF and IMRF, increased 1.8 to 1.9-fold between 1–6 dpl (Fig. 4A). One to five neurons in the area of NMLF were Bcl-2^{+}/tracer^{+} double-positive at 3 and 6 dpl (Figs. 4C–H) compared with unlesioned NMLF neurons (Fig. 4B). In the area of IMRF, 3–7 Bcl-2^{+}/tracer^{+} double-positive neurons could be seen at 3 and 6 dpl (Figs. 4J–O) compared with unlesioned IMRF neurons (Fig. 4I). In addition, the number of Bcl-2^{+} neurons was significantly increased at 3 dpl compared with unlesioned brainstem; from 8.7 ± 2.9 (n = 3) to 32.8 ± 2.2 (n = 4) in the NMLF ($p < 0.01$), and from 16.7 ± 3.3 (n = 3) to 55.8 ± 2.9 (n = 4) in the IMRF ($p < 0.001$).

A similar result was obtained for p-Akt in western blot analysis and immunohistochemistry. The expression of p-Akt protein in the brainstem increased approximately 2-fold between 1–6 dpl (Fig. 5A). In the area of NMLF and IMRF, 2–3 and 4–8 neurons were p-Akt^{+}/tracer^{+} double-positive at 3 and 6 dpl, respectively, compared with unlesioned NMLF and IMRF neurons (Figs. 5B–O). At 3 dpl, the number of p-Akt^{+} neurons significantly increased from 3.0 ± 0.6 (n = 3) to 26.0 ± 4.0 (n = 4) in the NMLF ($p < 0.01$), and from 8.3 ± 0.7 (n = 3) to 43.0 ± 9.4 (n = 4) in the IMRF ($p < 0.05$). These results showed that axotomized brainstem neurons survived for a long period owing to the increased expression of anti-apoptotic factors (Bcl-2 and p-Akt) over 3–6 dpl.

← Fig. 6

3.5. Axonal regeneration into the caudal part to the lesion site after SCI

To examine the capacity of axonal regeneration in zebrafish upper motor neurons after SCI, we made longitudinal sections (Fig. 6A-2) of the spinal cord at various time points after SCI, and performed hematoxylin-eosin (HE) staining and immunohistochemistry of GAP43 which is a maker of extending axons (Skene, 1989; Kaneda et al., 2008). HE staining revealed that thin fibers appeared to reconnect the transected spinal cord at 30 and 60 dpl (Figs. 6F and J). In the unlesioned spinal cord, no GAP43 immunoreactivity could be seen (Fig. 6A-1). At 15 dpl, a small number of $GAP43^+$ fibers were observed in the rostral part to the lesion site (Figs. 6B and D), but not in the caudal part (Figs. 6C and E). At 30 dpl, many $GAP43^+$ fibers were detected in the rostral part (Figs. 6G and H), with a few fibers in the caudal part (Figs. 6G and I). At 60 dpl, $GAP43^+$ axons increased both in the rostral and caudal part (Figs. 6K–M) to the lesion site compared with those at 30 dpl.

← Fig. 7

3.6. Recovery of motor function of zebrafish after SCI

To evaluate the recovery of motor function in zebrafish after SCI, we measured moving behavior in a three-dimensional fashion with a computer image processing system (Kato et al., 1996; Kato et al., 2004; Kaneda et al., 2008). The unlesioned fish can swim freely in an aquarium without any limitation (Fig. 7A). At 1 and 17 dpl, fish movement was dramatically impaired to 7% and 15% of the unlesioned fish, respectively (Figs. 7B and C). At 29 dpl, the swimming behavior increased to 31% of the unlesioned fish (Fig. 7D). At 53 dpl, the swimming behavior further increased to

54% of the unlesioned fish (Fig. 7E). Fig. 7F shows a temporal change of fish moving behavior between 1–52 dpl. The experiment was repeated 3–5 times.

4. Discussion

4.1. Long-term survival of upper motor neurons in the NMLF and IMRF of the adult zebrafish brainstem after SCI

Adult zebrafish are able to regenerate various tissues, including the CNS. In CNS regeneration, there are two cell sources of regenerating axons after injury. One is neurons differentiated from multipotent precursor cells, the other is the surviving neurons post-injury. In the present study using adult zebrafish, upper motor neurons in the NMLF and IMRF that were labeled by a neurotracer showed the upregulation of survival signaling for a long time after SCI. The survival of axotomized neurons was further confirmed by the absence of cell apoptosis and cell proliferation at any time after SCI (Figs. 2 and 3). Our data were in good agreement with previous findings in the adult zebrafish brain, reporting that the number of newly-generated neurons is extremely low in the region where descending neurons exist (Zupanc et al., 2005; Hinsch and Zupanc, 2007). In contrast to the upper motor neurons in the brainstem, motor neurons in the spinal cord become apoptotic after SCI, and neurogenesis from the ependymal zone around the central canal is activated via sonic hedgehog and/or Notch signaling (Reimer et al., 2008; Reimer et al., 2009; Dias et al., 2012).

In adult zebrafish retina, we have reported that the optic nerve can be restored, even after optic nerve transection, and visual function can be almost fully recovered within 90–100 days after axotomy (Kato et al., 2007; Kaneda et al., 2008). Similar to these studies, we have investigated the regenerative capacity of retinal ganglion cells (RGCs) after axotomy in the adult zebrafish, by comparing with the rat retina which cannot be regenerated. We have shown that there are no $TUNEL^+$ RGCs in the fish retina for at least 20 days after axotomy, whereas many $TUNEL^+$ RGCs were observed in the rat retina at 6 days after optic nerve crush (Koriyama et al., 2007; Homma et al.,

2007). Furthermore, the anti-apoptotic factors Bcl-2 and p-Akt are upregulated in the fish retina 2–5 days after axotomy, whereas these anti-apoptotic proteins are rapidly downregulated in the rat retina after nerve crush. The upregulation of Bcl-2 and p-Akt in the fish retina is mediated by the activation of the phosphatidylinositol-3-kinase/Akt signaling pathway through insulin-like growth factor-1 (IGF-1) (Koriyama et al., 2007; Jantas et al., 2009). In this study, we found that the levels of Bcl-2 and p-Akt increased rapidly in the brainstem approximately 2-fold between 1–6 days after SCI in adult zebrafish (Figs. 4 and 5), which was consistent with the increase in the number of Bcl-2- or p-Akt-positive cells in the NMLF and IMRF at 3 dpl compared with the unlesioned brainstem. And the increased expression of these anti-apoptotic factors was detected in retrogradely labeled neurons in the NMLF and IMRF. From these findings, it is suggested that axotomized neurons in the brainstem of adult zebrafish can survive after SCI through the upregulation of the anti-apoptotic factors, Bcl-2 and p-Akt. This is a new and convincing explanation for the survival of upper motor neurons following SCI in adult zebrafish.

4.2. Long distance regeneration of descending axons from upper motor neurons of the brainstem after SCI in adult zebrafish

In this study, we showed that long-distance regenerating axons descended beyond the lesion site of the spinal cord after SCI in adult zebrafish by three distinct methods. The first method is the double lesion test with a retrograde labeling: In this experiment, the fish received a primary lesion 4 mm caudal to the brainstem-spinal cord junction, and received a second lesion 4 mm caudal to the primary lesion site, to inject the retrograde tracer at 6 weeks after the initial lesion (Figs. 3H and I). A number of neurons in the NMLF and IMRF were labeled with a tracer injected at the second lesion

site (Figs. 3M and P; Becker et al., 1997). The second method was more direct: We used histology of longitudinal sections of the spinal cord to show that thin fibers connected the lesion site between 30–60 days after SCI (Fig. 6). In these longitudinal sections, we could see that there was an increase in the number of $GAP43^{+}$ axons in proportion to days after SCI. The third method used was to measure swimming behavior of zebrafish following SCI: Swimming behavior was measured three-dimensionally using a computer image processing system, which revealed that the temporal pattern of recovery of motor function is biphasic, with a slow recovery rate observed for first 2 weeks and a relatively fast recovery rate observed from 3–8 weeks after SCI (Fig. 7F). The turning point of these slow and fast phases is around 2 weeks after SCI, which corresponds well to the time taken for regenerating axons to reach the lesion site (Fig. 6). This three-dimensional behavior analysis revealed the recovery of motor function after SCI in more detail as compared to the previous study in which the two-dimensional tracking of fish was used (Becker et al., 2004). The biphasic pattern of behavioral recovery may be due to the increase in the number of $GAP43^{+}$ descending axons. Becker et al. (2005) further demonstrated that not only axotomized upper motor neurons but also intraspinal neurons upregulate GAP43 in response to SCI. At present, therefore, we cannot rule out the possibility that some of $GAP43^{+}$ axons shown in Fig. 6 are confused with regenerating intraspinal axons. However, as mentioned above, upper motor neurons could be retrogradely labeled from more caudal part to the lesion site at 6 weeks after SCI (Figs. 3M and P). Moreover, the swimming behavior was recovered in accordance with the increase of $GAP43^{+}$ axons in caudal part to the lesion site (Fig. 7). From these findings, it is certain that upper motor neurons can regenerate their axons across the lesion site following SCI. In spinal cord regeneration of adult zebrafish, it is known that motor neurons have regenerative capacity, but sensory neurons (e.g., dorsal

root ganglia) do not (Becker et al., 2005). It needs to be elucidated whether descending or ascending axons are present in the "bridge" connecting the proximal and distal segments in the vicinity of the lesion site. Furthermore, the exact molecular mechanism behind the axonal regeneration of brainstem neurons after SCI remains to be determined.

In optic nerve regeneration, we previously identified a variety of regeneration-associated genes and pathways involved in axonal elongation, such as retinoic acid signaling, retinal transglutaminase, and nitric oxide synthetase/NO signaling (Matsukawa et al., 2004; Sugitani et al., 2006; Koriyama et al., 2009; Nagashima et al., 2009; Sugitani et al., 2012). The next goal is to determine such regeneration-associated genes enabling upper motor neurons to regenerate their axons.

Acknowledgments

We would like to thank Ms. Sachiko Higashi and Ms. Tomoko Kano for their administrative and technical assistance. We also appreciate Drs. Catherina G. Becker, Thomas Becker and Tatyana B. Dias (Centre for Neuroregeneration, University of Edinburgh) for their expert technical advice. This work was supported in part by research grants from the Ministry of Education, Culture, Sports, Science and Technology, Japan (No. 23618006 to KS, No. 22791651 to YK and Nos. 22300109 and 23650163 to SK), and by Institutional Program for Young Researcher Overseas Visit Program of the Japan Society for the Promotion of Science (to KO).

References

Becker, T., Wullimann, M.F., Becker, C.G., Bernhardt, R.R., Schachner, M., 1997. Axonal regrowth after spinal cord transection in adult zebrafish. J. Comp. Neurol. 377, 577–595.

Becker, C.G., Lieberoth, B.C., Morellini, F., Feldner, J., Becker, T., Schachner, M., 2004. L1.1 is involved in spinal cord regeneration in adult zebrafish. J. Neurosci. 24, 7837–7842.

Becker, T., Lieberoth, B.C., Becker, C.G., Schachner, M., 2005. Differences in the regenerative response of neuronal cell populations and indications for plasticity in intraspinal neurons after spinal cord transection in adult zebrafish. Mol. Cell. Neurosci. 30, 265–278.

Dias, T.B., Yang, Y.J., Ogai, K., Becker, T., Becker, C.G., 2012. Notch signaling controls generation of motor neurons in the lesioned spinal cord of adult zebrafish. J. Neurosci. 32, 3245–3252.

Hains, B.C., Black, J.A., Waxman, S.G., 2003. Primary cortical motor neurons undergo apoptosis after axotomizing spinal cord injury J. Comp. Neurol. 462, 328–341.

Hinsch, K, Zupanc, G.K., 2007. Generation and long-term persistence of new neurons in the adult zebrafish brain: a quantitative analysis. Neuroscience 146, 679–696.

Homma, K., Koriyama, Y., Mawatari, K., Higuchi, Y., Kosaka, J., Kato, S., 2007. Early downregulation of IGF-I decides the fate of rat retinal ganglion cells after optic nerve injury. Neurochem. Int. 50, 741–748.

Jantas, D., Szymanska, M., Budziszewska, B., Lason, W., 2009. An involvement of BDNF and PI3-K/Akt in the anti-apoptotic effect of memantine on staurosporine-evoked cell death in primary cortical neurons. Apoptosis 14, 900–912.

Kaneda, M., Nagashima, M., Nunome, T., Muramatsu, T., Yamada, Y., Kubo, M., Muramoto, K., Matsukawa, T., Koriyama, Y., Sugitani, K., Vachkov, I.H., Mawatari, K., Kato, S., 2008. Changes of phospho-growth-associated protein 43 (phospho-GAP43) in the zebrafish retina after optic nerve injury: a long-term observation. Neurosci. Res. 61, 281–288.

Kato, S., Tamada, K., Shimada, Y., Chujo, T., 1996. A quantification of goldfish behavior by an image processing system. Behav. Brain. Res. 80, 51–55.

Kato, S., Nakagawa, T., Ohkawa, M., Muramoto, K., Oyama, O., Watanabe, A., Nakashima, H., Nemoto, T., Sugitani, K., 2004. A computer image processing system for quantification of zebrafish behavior. J. Neurosci. Methods. 134, 1–7.

Kato, S., Koriyama, Y., Matsukawa, T., Sugitani, K., 2007. Optic nerve regeneration in goldfish. In: Becker, C.G., Becker, T. (Eds.), Model Organisms in Spinal Cord Regeneration. Wiley-VCH, Germany, pp. 355–372.

Kizil, C., Kaslin, J., Kroehne, V., Brand, M., 2012. Adult neurogenesis and brain regeneration in zebrafish. Dev. Neurobiol. 72, 429–461.

Koriyama, Y., Homma, K., Sugitani, K., Higuchi, Y., Matsukawa, T., Murayama, D., Kato, S., 2007. Upregulation of IGF-I in the goldfish retinal ganglion cells during the early stage of optic nerve regeneration. Neurochem. Int. 50, 749–756.

Koriyama, Y., Ohno, M., Kimura, T., Kato, S., 2009. Neuroprotective effects of 5-S-GAD against oxidative stress-induced apoptosis in RGC-5 cells. Brain. Res. 1296, 187–195.

Matsukawa, T., Sugitani, K., Mawatari, K., Koriyama, Y., Liu, Z., Tanaka, M., Kato, S., 2004. Role of purpurin as a retinol-binding protein in goldfish retina during the early stage of optic nerve regeneration: its priming action on neurite outgrowth. J. Neurosci. 24, 8346–8353.

Nagashima, M., Sakurai, H., Mawatari, K., Koriyama, Y., Matsukawa, T., Kato, S., 2009. Involvement of retinoic acid signaling in goldfish optic nerve regeneration. Neurochem. Int. 54, 229–236.

Reimer, M.M., Sörensen, I., Kuscha, V., Frank, R.E., Liu, C., Becker, C.G., Becker, T., 2008. Motor neuron regeneration in adult zebrafish. J. Neurosci. 28, 8510–8516.

Reimer, M.M., Kuscha, V., Wyatt, C., Sörensen, I., Frank, R.E., Knüwer, M., Becker, T., Becker, C.G., 2009. Sonic hedgehog is a polarized signal for motor neuron regeneration in adult zebrafish. J. Neurosci. 29, 15073–15082.

Skene, J.H., 1989. Axonal growth-associated proteins. Annu. Rev. Neurosci. 12, 127–156.

Sugitani, K., Matsukawa, T., Koriyama, Y., Shintani, T., Nakamura, T., Noda, M., Kato, S., 2006. Upregulation of retinal transglutaminase during the axonal elongation stage of goldfish optic nerve regeneration. Neuroscience 142, 1081–1092.

Sugitani, K., Ogai, K., Hitomi, K., Nakamura-Yonehara, K., Shintani, T., Noda, M., Koriyama, Y., Matsukawa, T., Kato, S., 2012. A distinct effect of transient and sustained upregulation of cellular factor XIII in the goldfish retina and optic nerve on optic nerve regeneration. Neurochem. Int. In press.

Van Raamsdonk, W., Maslam, S., de Jong, D.H., Smit-Onel, M.J., Velzing, E., 1998. Long term effects of spinal cord transection in zebrafish: swimming performances, and metabolic properties of the neuromuscular system. Acta. Histochem. 100, 117–131.

Wullimann, M.F., Rupp, B., Reichert, H., 1996. Neuroanatomy of the Zebrafish Brain: A Topological Atlas, first ed. Birkhäuser Basel, Berlin.

Zupanc, G.K., Hinsch, K., Gage, F.H., 2005. Proliferation, migration, neuronal differentiation, and long-term survival of new cells in the adult zebrafish brain. J.

Comp. Neurol. 488, 290–319.

Figure captions

Fig. 1

Stable retrograde labeling of brainstem neurons after SCI in adult zebrafish. (A) Sagittal and coronal schemes of the adult zebrafish brain. Shaded areas depict the position of the NMLF. (B–D) Rhodamine dextran amine (RDA), a neurotracer, could be detected at 1 (B), 3 (C) and 6 dpl (D) in coronal sections of the NMLF. About 10 neurons were retrogradely labeled from the lesion site. (E) The position of the IMRF. (F–H) Approximately 8–10 neurons were labeled in the coronal section of the IMRF at 1 (F), 3 (G) and 6 dpl (H). Scale bars, 100 μm for B–D and F–H.

Fig. 2

Absence of apoptosis in axotomized brainstem neurons of the NMLF and IMRF after SCI in adult zebrafish. TUNEL assay images, with retrograde tracer and TUNEL/tracer/DAPI overlay in the NMLF (A–C) and IMRF (D–F) at 6 dpl are shown. A number of tracer^{+} neurons could be seen in the NMLF (B) and IMRF (E), whereas no TUNEL^{+} signal was detected in these nuclei (A, C, D and F). Solid arrowheads highlight the TUNEL^{-}/tracer^{+} neurons, and open arrowheads highlight the non-specific signals. The image in the open square was enlarged and placed as an inset image for each panel. Scale bars, 50 μm (inset, 10 μm).

Fig. 3

Absence of cell proliferation in the area of the NMLF and IMRF after SCI in adult zebrafish. (A) The time course of the short-term experiment. BrdU was injected intraperitoneally at 0, 2 and 4 dpl and immunohistochemistry for BrdU was performed

at 7 dpl. (B and C) In the paraventricular zone of the telencephalon, where the signals of neurogenesis can be seen even in the adult, there were a number of $BrdU^+$ cells, indicating that the incorporation of BrdU was successful. (D–G) In the NMLF (D and E) and IMRF (F and G) of the same subject as (B) and (C), there were no $BrdU^+$ cells. (H and I) The layout of the long-term experiment. BrdU was injected at 0, 2 and 4 dpl, and at 6 weeks (42 days) after SCI, biocytin was applied 4 mm caudal to the initial lesion site to label the neurons in the NMLF and IMRF. The sections were prepared at 43 dpl, 1 day after tracer application. (J and K) BrdU incorporation was confirmed by the positive signals in the telencephalic area. (L–Q) Even at 42 dpl, there were no $BrdU^+$ cells in the NMLF (L) and IMRF (O). However, many $tracer^+$ neurons could be seen in these areas (M and P), and all of which were $BrdU^-$ (N and Q). Solid arrowheads mark the $BrdU^-/tracer^+$ neurons, and open arrowheads mark the non-specific signals. The image in the open square was enlarged and placed as an inset image for each panel. Scale bars, 50 μm (inset, 10 μm).

Fig. 4

Upregulation of the anti-apoptotic factor Bcl-2 in axotomized brainstem neurons of the NMLF and IMRF after SCI in adult zebrafish. (A) Western blot analysis of Bcl-2 protein revealed that expression of Bcl-2 increased approximately 1.8-fold at 1–6 dpl. Equal amounts of protein were loaded in each lane of the gel, confirmed by CBB staining. (B–H) Images of Bcl-2 immunohistochemistry and retrograde tracing in the NMLF. At 3 and 6 dpl, 1–5 neurons were retrogradely labeled (D and G), and these neurons were colocalized with Bcl-2 (C, E, F and H) compared with the unlesioned NMLF neurons (B). (I–O) Bcl-2 immunohistochemistry in the IMRF. Similar to the NMLF, there were 3–7 $tracer^+$ neurons (K and N) with $Bcl\text{-}2^+$ (J, L, M and O) compared

with unlesioned IMRF neurons (I). Solid arrowheads mark the Bcl-2^{+}/tracer^{+} neurons. Neurons in an open square were magnified and placed as the inset. Scale bars, 100 μm (inset, 20 μm).

Fig. 5

Upregulation of the anti-apoptotic factor p-Akt in axotomized brainstem neurons of the NMLF and IMRF after SCI in adult zebrafish. (A) The increase in p-Akt protein levels of approximately 2-fold occurred from 1 dpl compared with the unlesioned brainstem. (B–H) Immunohistochemistry of p-Akt in the NMLF. There were 2–3 retrogradely labeled neurons in the NMLF (D and G) which were also p-Akt^{+} (C, E, F and H). (I–O) Immunohistochemistry of p-Akt in the IMRF. Four to eight neurons, which were retrogradely labeled with the tracer (K and N), were also p-Akt^{+} (J, L, M and O). Solid arrowheads mark the p-Akt^{+}/tracer^{+} neurons. Neurons in an open square were magnified and placed as the inset. Scale bars, 100 μm (inset, 20 μm).

Fig. 6

Regeneration of descending axons extending beyond the lesion site of the spinal cord after SCI in adult zebrafish. Hematoxylin-eosin (HE) staining and GAP43 immunohistochemistry were performed in longitudinal sections of unlesioned (A-1) and lesioned (B–M) spinal cord. The orientation of the longitudinal section is shown in (A-2). (A-1) In unlesioned spinal cord, there were no GAP43^{+} fibers. At 15 dpl, a few GAP43^{+} fibers could be seen in the rostral part to the lesion site (B and D), whereas no GAP43^{+} fibers were detected in the caudal part (C and E). At 30 dpl, there were more GAP43^{+} fibers in the rostral part (G and H) compared with 15 dpl. In addition, there were a few GAP43^{+} fibers in the caudal part (G and I). At 60 dpl, there were a number

of GAP43^{+} fibers both in the rostral and the caudal part to the lesion site (K–M). HE staining revealed that a thin “bridge” was formed at the lesion site at 30 and 60 dpl (F and J). Arrows indicate the lesion site. Scale bars, 500 μm for A, B, C, F, G, J and K, 100 μm for D, E, H, I, L and M.

Fig. 7

Three-dimensional behavior analysis of freely-moving zebrafish after SCI. Spontaneous swimming of the fish was traced for 5 min, and total swimming distance was calculated. (A–E) Representative three-dimensional trackings of the fish. The unlesioned fish can swim unrestrictedly (A). However, the swimming capability was significantly impaired at 1, 17 and 29 dpl (B, C and D, respectively), although gradual recovery was observed. At 53 dpl (E), there was a steep recovery in the distance swam to about 54% of the unlesioned fish, which is not significantly different. (F) Temporal changes of swimming distance after SCI. Values in (F) are expressed as the means ± SEM. *$p < 0.05$, **$p < 0.01$, compared with the unlesioned fish. n. s.: not significant. n = 3–5 in each timepoint. Scale bars (shown next to the scheme (A)) for A–E, 10 cm in each direction.

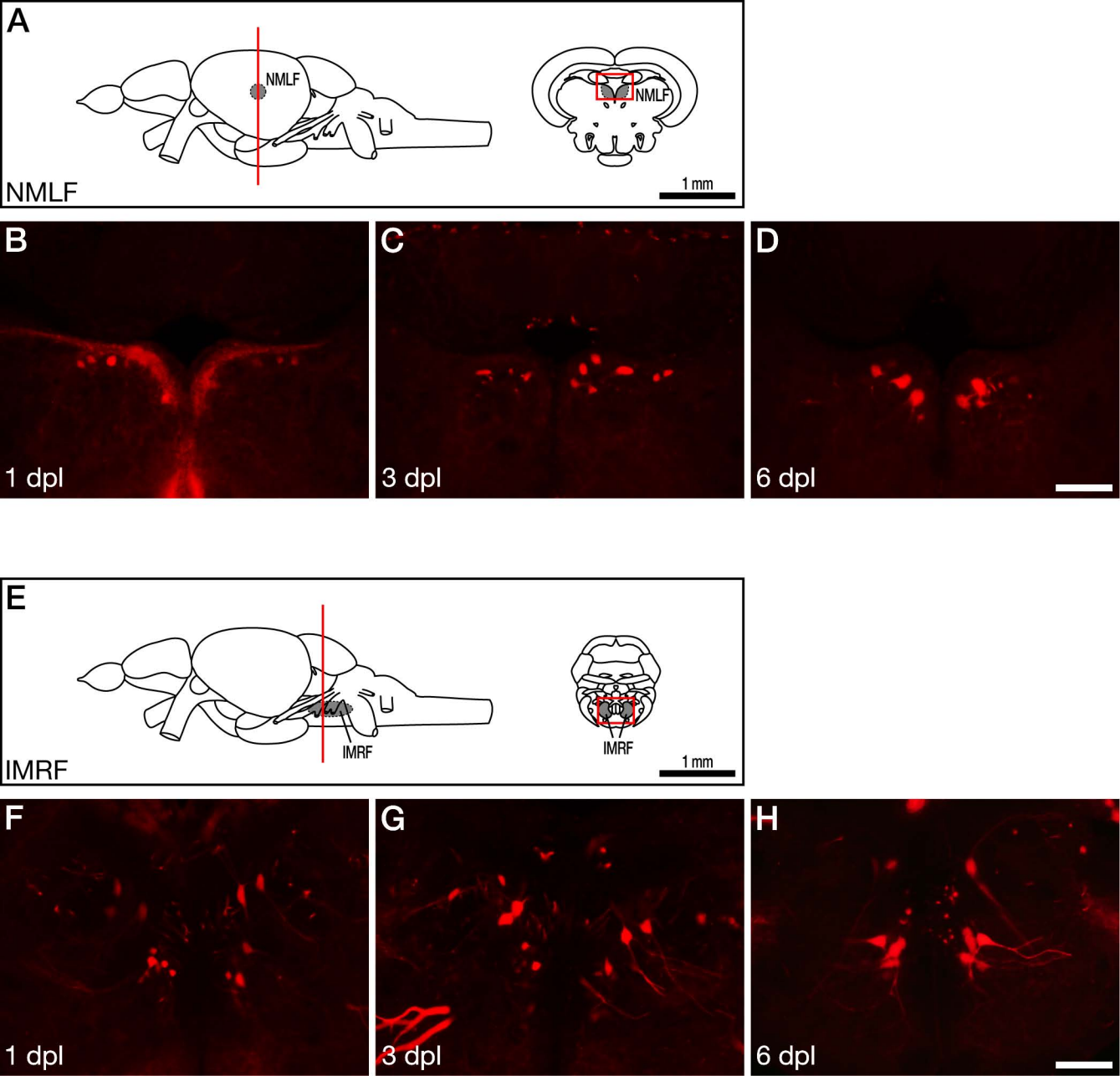
A
NMLF
NMLF
NMLF
1 mm
B
1 dpl
C
3 dpl
D
6 dpl
E
IMRF
IMRF
IMRF
1 mm
F
1 dpl
G
3 dpl
H
6 dpl

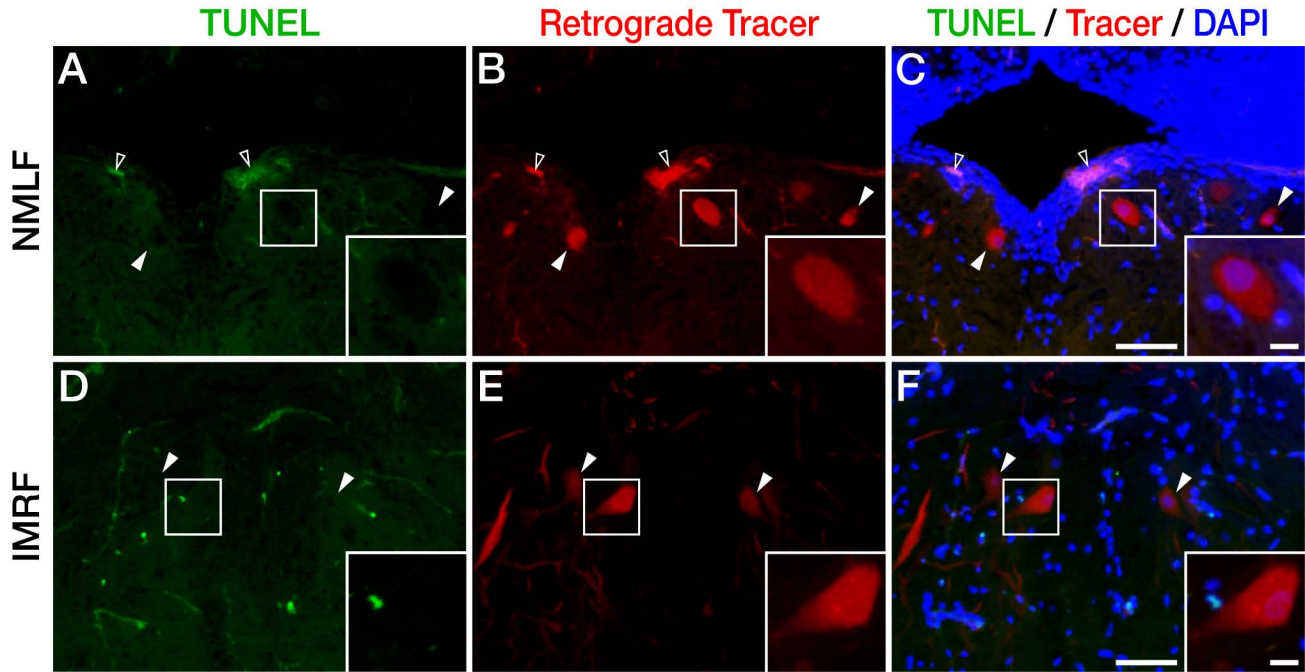
TUNEL
Retrograde Tracer
TUNEL / Tracer / DAPI
NMLF
IMRF
A
B
C
D
E
F

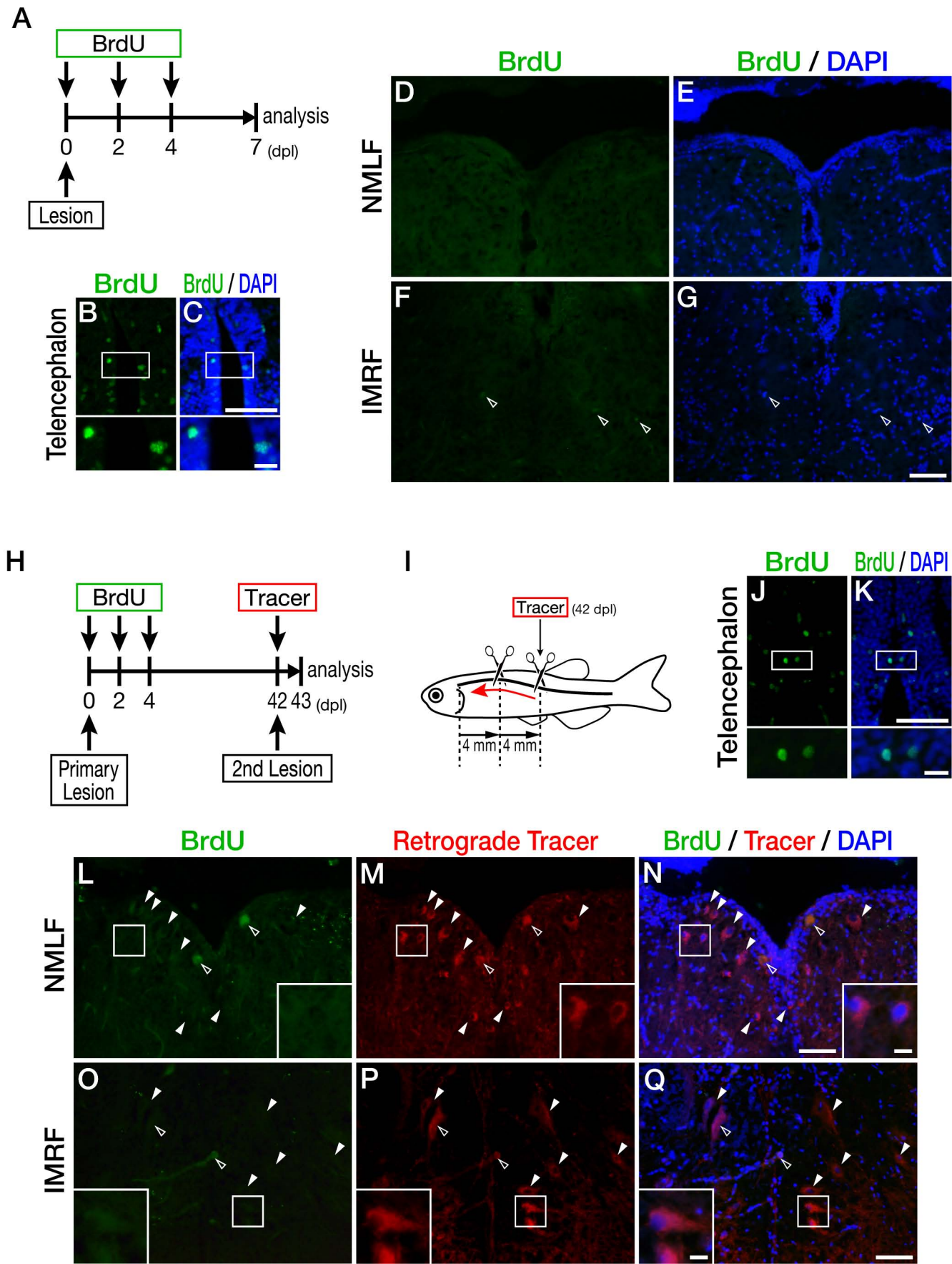
A
BrdU
analysis
0
2
4
7 (dpl)
Lesion
BrdU
BrdU / DAPI
Telencephalon
B
C
BrdU
BrdU / DAPI
NMLF
D
E
IMRF
F
G
H
BrdU
Tracer
analysis
0 2 4
42 43 (dpl)
Primary Lesion
2nd Lesion
I
Tracer (42 dpl)
4 mm
4 mm
BrdU
BrdU / DAPI
Telencephalon
J
K
BrdU
Retrograde Tracer
BrdU / Tracer / DAPI
NMLF
L
M
N
IMRF
O
P
Q

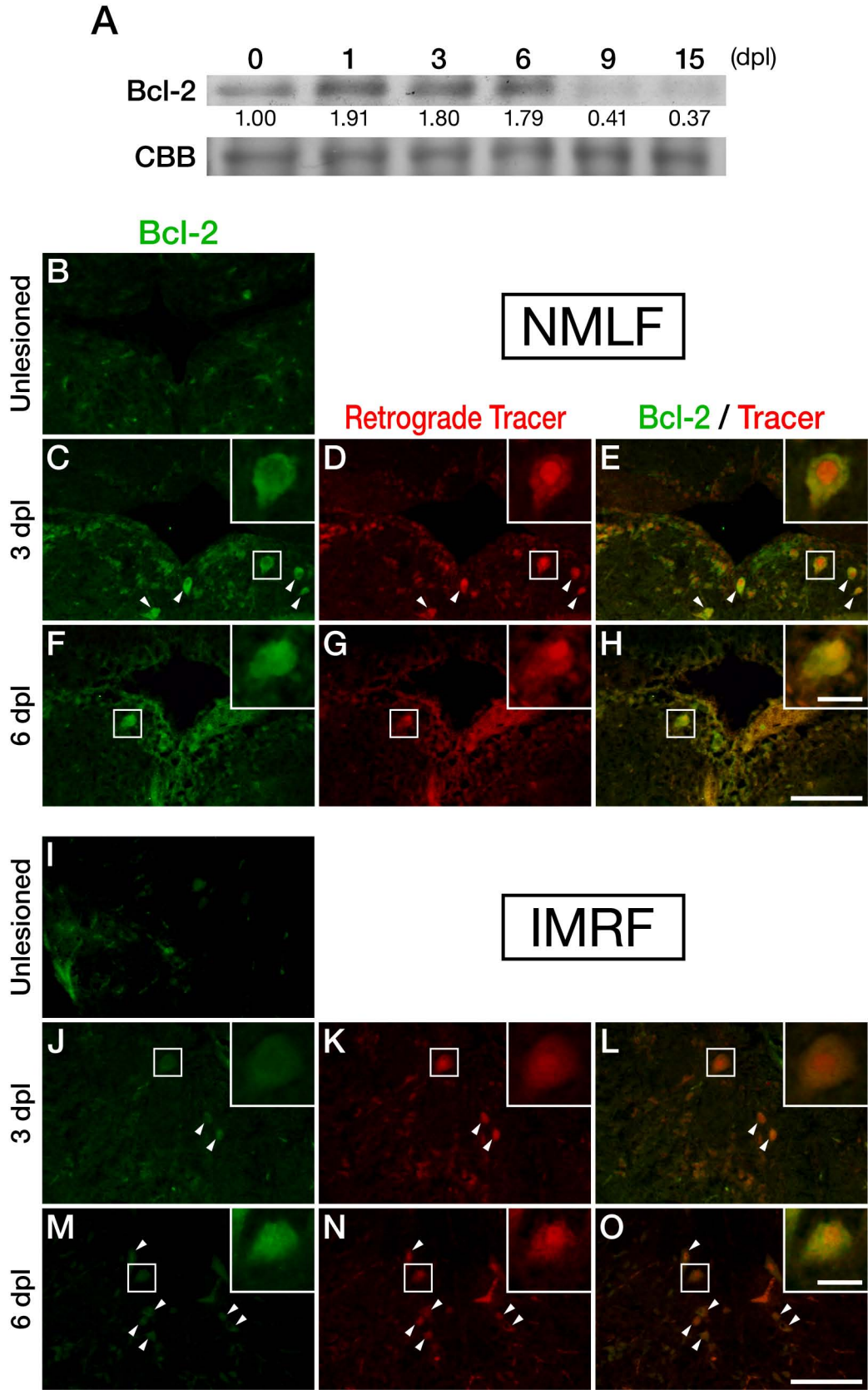
A
0
1
3
6
9
15
(dpl)
Bcl-2
1.00
1.91
1.80
1.79
0.41
0.37
CBB
Bcl-2
Unlesioned
B
NMLF
Retrograde Tracer
Bcl-2 / Tracer
3 dpl
C
D
E
6 dpl
F
G
H
Unlesioned
I
IMRF
3 dpl
J
K
L
6 dpl
M
N
O

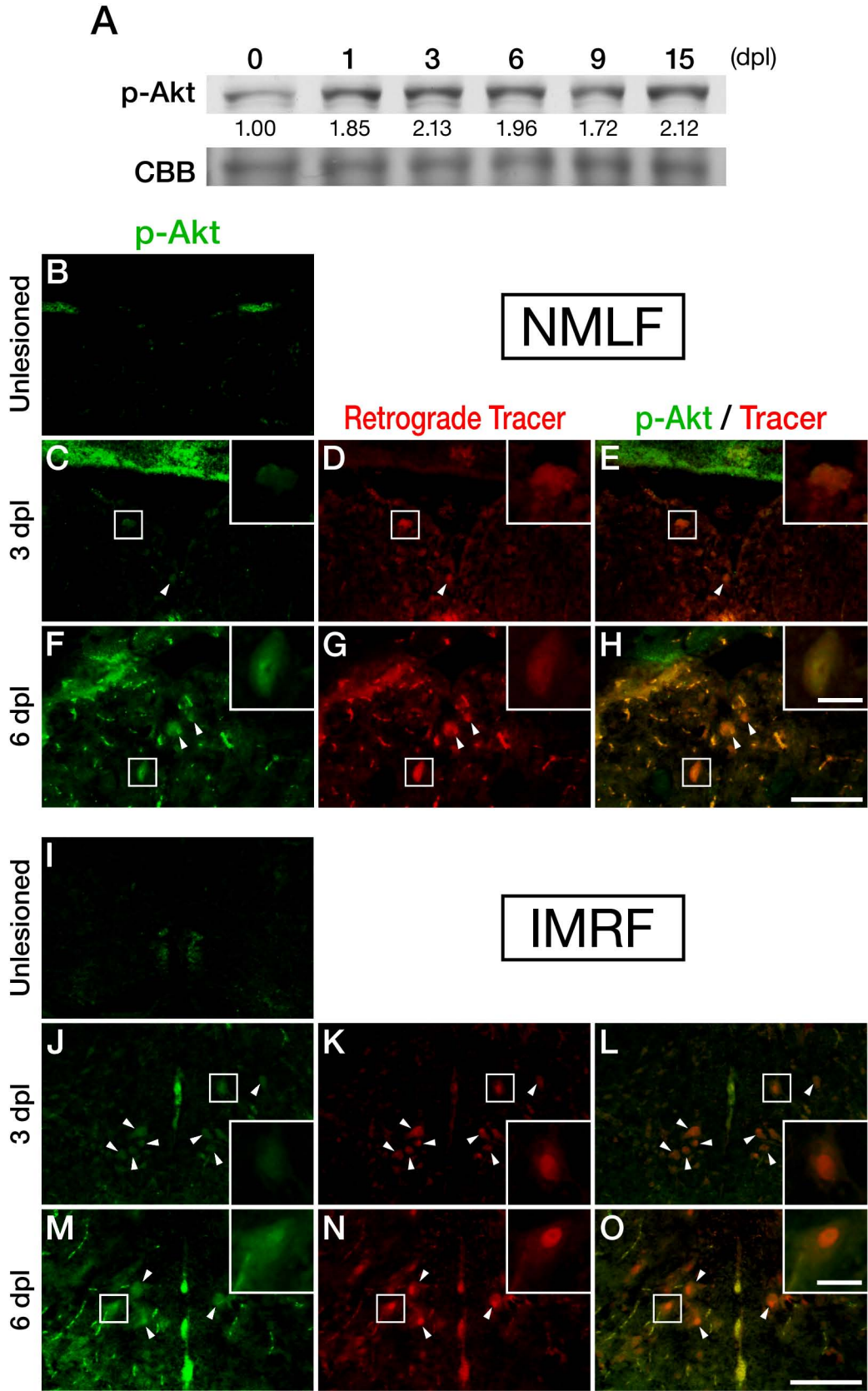
A
0
1
3
6
9
15
(dpl)
p-Akt
1.00
1.85
2.13
1.96
1.72
2.12
CBB
p-Akt
Unlesioned
B
NMLF
Retrograde Tracer
p-Akt / Tracer
3 dpl
C
D
E
6 dpl
F
G
H
Unlesioned
I
IMRF
3 dpl
J
K
L
6 dpl
M
N
O

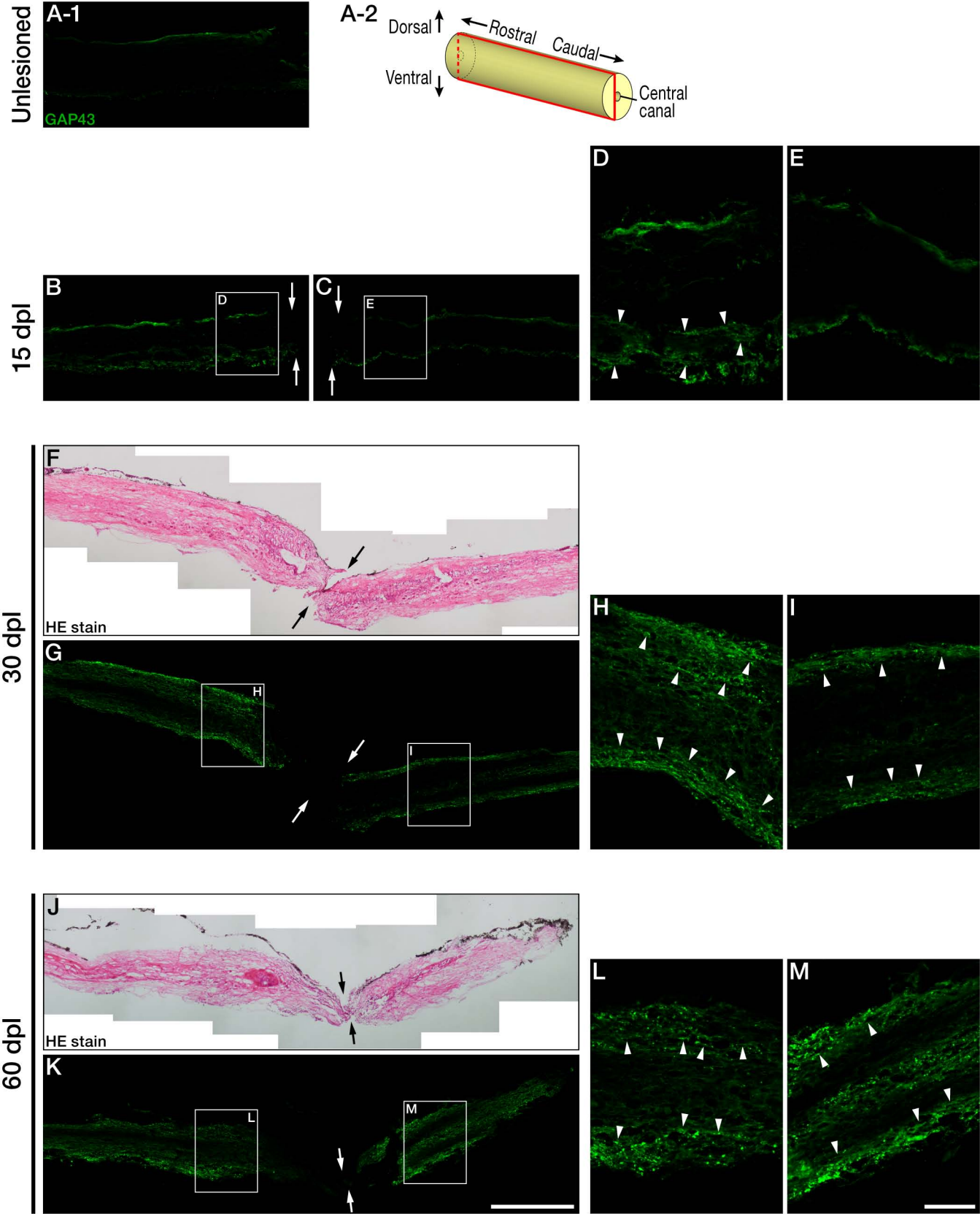
Unlesioned
A-1
GAP43
A-2
Dorsal
Rostral
Caudal
Ventral
Central canal
15 dpl
B
D
C
E
D
E
30 dpl
F
HE stain
G
H
I
H
I
60 dpl
J
HE stain
K
L
M
L
M